This article was downloaded by: [Renmin University of China]
On: 13 October 2013, At: 10:42
Publisher: Taylor & Francis
Informa Ltd Registered in England and Wales Registered Number: 1072954 Registered office: Mortimer House, 37-41 Mortimer Street, London W1T 3JH, UK

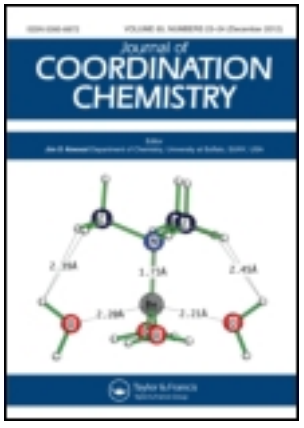

Journal of Coordination Chemistry
Publication details, including instructions for authors and subscription information:
http://www.tandfonline.com/loi/gcoo20

Syntheses and crystal structures of four new fpa-metal complexes through in situ ligand reaction

Jiang-Feng Song [a], Jia Zhang [a], Rui-Sha Zhou [a], Li Sun [a], Tuo-Ping Hu [a] & Qiao-Ling LI [a]

[a] Department of Chemistry, North University of China, Taiyuan, Shanxi 030051, P.R. China

Accepted author version posted online: 17 Oct 2012.Published online: 01 Nov 2012.

To cite this article: Jiang-Feng Song, Jia Zhang, Rui-Sha Zhou, Li Sun, Tuo-Ping Hu & Qiao-Ling LI (2012) Syntheses and crystal structures of four new fpa-metal complexes through in situ ligand reaction, Journal of Coordination Chemistry, 65:24, 4375-4388, DOI: 10.1080/00958972.2012.740557

To link to this article: http://dx.doi.org/10.1080/00958972.2012.740557

PLEASE SCROLL DOWN FOR ARTICLE

Taylor & Francis makes every effort to ensure the accuracy of all the information (the "Content") contained in the publications on our platform. However, Taylor & Francis, our agents, and our licensors make no representations or warranties whatsoever as to the accuracy, completeness, or suitability for any purpose of the Content. Any opinions and views expressed in this publication are the opinions and views of the authors, and are not the views of or endorsed by Taylor & Francis. The accuracy of the Content should not be relied upon and should be independently verified with primary sources of information. Taylor and Francis shall not be liable for any losses, actions, claims, proceedings, demands, costs, expenses, damages, and other liabilities whatsoever or howsoever caused arising directly or indirectly in connection with, in relation to or arising out of the use of the Content.

This article may be used for research, teaching, and private study purposes. Any substantial or systematic reproduction, redistribution, reselling, loan, sub-licensing, systematic supply, or distribution in any form to anyone is expressly forbidden. Terms &

Conditions of access and use can be found at http://www.tandfonline.com/page/terms-and-conditions

Downloaded by [Renmin University of China] at 10:42 13 October 2013

Journal of Coordination Chemistry
Vol. 65, No. 24, 20 December 2012, 4375–4388

Taylor & Francis
Taylor & Francis Group

Syntheses and crystal structures of four new fpa-metal complexes through *in situ* ligand reaction

JIANG-FENG SONG*, JIA ZHANG, RUI-SHA ZHOU, LI SUN, TUO-PING HU and QIAO-LING LI

Department of Chemistry, North University of China, Taiyuan, Shanxi 030051, P.R. China

(*Received 19 March 2012; in final form 7 September 2012*)

Four new fpa-metal complexes, $[Co(fpa)_2(H_2O)_2]$ (**1**), $[Cu(fpa)_2(H_2O)]$ (**2**), $[Zn_2(fpa)_4(bpp)_2]_n$ (**3**), and $\{[Zn(bpy)(H_2O)_4]\cdot 2(fpa)\}_n$ (**4**), have been synthesized and fully characterized by elemental analyses, IR spectroscopy, single-crystal X-ray diffraction, and thermogravimetric analysis (TGA), (Hfpa = 2,2-difluoro-2-(pyridine-2-yl)acetate, bpp = 1,3-bis(4-pyridyl)propane, bpy = 4,4′-bipyridine). X-ray diffraction analyses reveal that **1** and **2** with 0-D structures are both extended into 3-D supramolecular networks through hydrogen bonds and $\pi\cdots\pi$ interactions. Complex **3** with chiral centers possesses a 1-D structure constructed by two kinds of bpp molecules and four kinds of fpa^- molecules with different conformations, with bbp and fpa^- bridging and capped ligands, respectively. In **4**, bpy links $[Zn(H_2O)_4]^{2+}$ into a 1-D polymeric cationic chain and uncoordinated fpa^- compensates the framework charge. The results of TGA reveal that fpa^- decomposes through two processes. Both **3** and **4** show strong fluorescence in the solid state at room temperature.

Keywords: Hydrogen bonds; Coordination complex; Crystal structure; *In situ* reaction

Downloaded by [Renmin University of China] at 10:42 13 October 2013

1. Introduction

Coordination complexes have attracted attention due to their structures and wide applications in storage, separation, catalysis, biomedical and sensor materials, etc. [1–13]. Although promising results have been achieved and startling applications have been developed, the rational design and synthesis of coordination complexes with unique structure and function still remain a long-term challenge because self-assembly is often influenced by medium, the nature of the ligands, pH of solution, temperature, metal coordination environments, etc. [14–21]. The ligand is one of the most important factors to construct coordination polymers. Coordination mode and competitive reaction with auxiliary ligands is important for targeted organic linkers.

Coordination polymers *via* 2-pyridinecarboxylic acid or its derivatives have drawn attention [22–28]; however, coordination chemistry of 2,2-difluoro-2-(pyridin-2-yl)acetate (Hfpa), similar to 2-pyridinecarboxylic acid, is less. The choice of Hfpa is based on the following considerations: (1) it contains two distinct coordination sites involving carboxylic groups and pyridine creating multiple possible binding sites; (2) it

*Corresponding author. Email: jfsong0129@gmail.com

ISSN 0095-8972 print/ISSN 1029-0389 online © 2012 Taylor & Francis
http://dx.doi.org/10.1080/00958972.2012.740557

is expected to assemble novel structural motifs due to the different coordination modes and molecular conformations; (3) strong induction of two fluorines can change coordination activity of Hfpa; and (4) fluorine and the aromatic ring in Hfpa might be involved in supramolecular recognition, such as C–F···H, C–F···π, and $\pi\cdots\pi$ interactions [29].

This study investigates the effect of coordination mode and competitive reaction with auxiliary organic linkers on formation of different structures. Here, we report synthesis, crystal structures of four new complexes constructed by Hfpa, $[Co(fpa)_2(H_2O)_2]$ (**1**), $[Cu(fpa)_2(H_2O)]$ (**2**), $[Zn_2(fpa)_4(bpp)_2]_n$ (**3**), and $\{[Zn(bpy)(H_2O)_2]\cdot 2(fpa)\}_n$ (**4**) as comparison to two reported complexes $[Cd(phen)Cl_2]_n$ (**5**) and $[Ni(bimb)_2Cl_2]_n$ (**6**) (phen = 1,10-phenanthroline and bimb = 1,4-bis(imidazol-1-yl)-butane) [30, 31]. Both **1** and **2** are extended into 3-D supramolecular networks through hydrogen bonds and $\pi\cdots\pi$ interactions. In **3**, bpp links Zn ions into a 1-D polymeric chain, in which unidentate fpa^- is an effective capped ligand. In **4**, bpy links $[Zn(H_2O)_4]^{2+}$ into a 1-D polymeric cationic chain and uncoordinated fpa^- compensates framework charge.

2. Experimental

2.1. *Materials and methods*

All chemicals and solvents were of reagent grade and used without purification; ethyl 2,2-difluoro-2-(pyridin-2-yl)acetate (Efpa) was selected as Hfpa source. Elemental analyses (C, H, and N) were performed on a Perkin-Elmer 240 C elemental analyzer. IR spectrum was measured on a Perkin-Elmer Spectrum One FT-IR spectrometer using KBr pellets. Thermogravimetric analysis (TGA) was performed on a Perkin-Elmer TGA-7000 thermogravimetric analyzer under flowing air at a temperature ramp rate of $10^\circ C\,min^{-1}$. Fluorescence spectra were obtained on a LS 55 fluorescence/phosphorescence spectrophotometer at room temperature.

2.2. *Syntheses of 1–5*

2.2.1. Synthesis of 1. A solution of Efpa (10.0 mg, 0.05 mmol) in 5 mL ethanol was directly mixed with a solution of $CoCl_2$ in 1 mL water ($0.10\,mol\,dm^{-3}$) in a 15 mL beaker at room temperature. The resulting mixed solution was transferred and sealed in a 25 mL Teflon-lined stainless steel reactor and heated at 85°C for 72 h. Upon cooling to room temperature, light red crystals were filtered and washed with water and ethanol. Yield: 62% (based on Efpa). Elemental Anal. Calcd for $C_{14}H_{12}CoF_4N_2O_6$ (439.19): C, 38.25; H, 2.73; N, 6.38. Found: C, 38.34; H, 2.75; N, 6.35. IR data (KBr, cm^{-1}): 3384(s), 2947(w), 1650(s), 1398(s), 1283(m), 1164(s), 1116(m), 1028(m), 812(m), 763(m), 694(m).

2.2.2. Synthesis of 2. The procedure was the same as that for **1** except that $CoCl_2$ was replaced by $CuSO_4$ ($0.10\,mol\,dm^{-3}$). The light blue crystals were filtered and washed with water and ethanol. Yield: 68% (based on Efpa). Elemental Anal.

Downloaded by [Renmin University of China] at 10:42 13 October 2013

Calcd for $C_{14}H_{10}CuF_4N_2O_5$ (425.78): C, 39.46; H, 2.35; N, 6.58. Found: C, 39.34; H, 2.35; N, 6.55. IR data (KBr, cm^{-1}): 3380(m), 2945(w), 1681(s), 1380(s), 1284(m), 1172(s), 1077(s), 835(m), 773(m), 698(m).

2.2.3. Synthesis of 3. A solution of Efpa (10.0 mg, 0.05 mmol) in 2 mL ethanol was directly mixed with a solution of $ZnCl_2$ in 1 mL water (0.10 mol dm^{-3}) in a 15 mL beaker at room temperature. A solution of bpp (10.0 mg, 0.05 mmol) in 3 mL ethanol in another 15 mL beaker was added to the mixture. Then 2 molL^{-1} HCl was added until the pH of the mixture is 5.0. The resulting mixed solution was transferred and sealed in a 25 mL Teflon-lined stainless steel reactor and heated at 85°C for 72 h. Upon cooling to room temperature, light yellow crystals were filtered and washed with water and ethanol. Yield: 32% (based on Efpa). Elemental Anal. Calcd for $C_{54}H_{44}F_8N_8O_8Zn_2$ (1215.71): C, 53.30; H, 3.62; N, 9.21. Found: C, 53.34; H, 3.65; N, 9.25. IR data (KBr, cm^{-1}): 3310(m), 3106(m), 2947(w), 1599(s), 1518(s), 1413(s), 1087(s), 1005(m), 866(m), 788(s), 694(m), 625(m).

2.2.4. Synthesis of 4. The procedure was the same as that for **3** except that bpp was replaced by bpy (7.4 mg, 0.05 mmol). Colorless crystals were filtered and washed with water and ethanol. Yield: 42% (based on Efpa). Elemental Anal. Calcd for $C_{24}H_{24}F_4N_4O_8Zn$ (637.84): C, 45.15; H, 3.76; N, 8.78. Found: C, 45.14; H, 3.79; N, 8.75. IR data (KBr, cm^{-1}): 3373(s), 1643(s), 1403(s), 1273(m), 1135(s), 1077(m), 1008(m), 812(m), 751(m), 686(m), 626(m).

2.2.5. Synthesis of 5. The procedure was the same as that for **3** except that bpp and $ZnCl_2$ were replaced by phen and $CdCl_2$. Colorless crystals were filtered and washed with water and ethanol. Yield: 63% (based on Efpa). IR data (KBr, cm^{-1}): 2945(w), 1413(w), 1243(m), 1093(m), 1046(m), 1002(w), 989(s), 866(s).

2.3. *Crystal structure determination*

The crystal structures were determined by single-crystal X-ray diffraction. Reflection data were collected on a Bruker SMART CCD area-detector diffractometer (Mo-Kα radiation, graphite monochromator) at room temperature with the ω-scan mode. Empirical adsorption correction was applied to all data using SADABS. The structures were solved by direct methods and refined by full-matrix least squares on F^2 using SHELXTL 97 [32]. Non-hydrogen atoms were refined anisotropically. Hydrogen atoms were located from difference maps and refined as riding, with O–H 0.85 in **1**–**4**. All calculations were carried out using SHELXTL 97 [32] and PLATON [33]. The crystallographic data and pertinent information are given in table 1; selected bond lengths and angles in table 2; and geometric parameters of hydrogen bonds in table 3.

Downloaded by [Renmin University of China] at 10:42 13 October 2013

Downloaded by [Renmin University of China] at 10:42 13 October 2013

Table 1. Crystal and structure refinement data for **1–4**.

Compound	**1**	**2**	**3**	**4**
Empirical formula	$C_{14}H_{12}CoF_4N_2O_6$	$C_{14}H_{10}CuF_4N_2O_5$	$C_{54}H_{44}F_8N_8O_8Zn_2$	$C_{24}H_{24}F_4N_4O_8Zn$
Formula weight	439.19	425.78	1215.71	637.84
Crystal system	Monoclinic	Orthorhombic	Monoclinic	Monoclinic
Space group	*C*2/*c*	*Pbcn*	$P2_1$	*C*2/*c*
Unit cell dimensions (Å, °)				
a	9.946(2)	14.175(3)	13.709(3)	14.7597(6)
b	24.727(5)	12.286(3)	13.644(3)	11.4875(4)
c	13.848(3)	9.0724(18)	14.811(3)	15.2916(6)
α	90	90	90	90
β	96.60(3)	90.00(3)	109.85(3)	93.8340(10)
γ	90	90	90	90
Volume (Å^3), *Z*	3383.1(12), 8	1580.1(5), 4	2605.8(9), 2	2586.92(17), 4
Calculated density (g cm^{-3})	1.725	1.790	1.549	1.638
Absorption coefficient (mm^{-1})	1.092	1.457	1.013	1.035
θ range for data collection (°)	3.22–27.48	3.14–27.48	3.00–27.46	2.25–28.28
Reflections collected	16,462	14,393	24,929	7952
Unique reflections	3868 [*R*(int) = 0.0445]	1810 [*R*(int) = 0.0391]	11,597 [*R*(int) = 0.0432]	3161 [*R*(int) = 0.0133]
Completeness to θ (%)	99.6	99.9	99.4	97.9
Goodness-of-fit on F^2	1.027	1.064	0.972	1.035
R indexes [$I > 2\sigma(I)$][a]	$R_1 = 0.0317$, $wR_2 = 0.0667$	$R_1 = 0.0285$, $wR_2 = 0.0726$	$R_1 = 0.0455$, $wR_2 = 0.1067$	$R_1 = 0.0242$, $wR_2 = 0.0649$
R (all data)[a]	$R_1 = 0.0442$, $wR_2 = 0.0714$	$R_1 = 0.0396$, $wR_2 = 0.0771$	$R_1 = 0.0737$, $wR_2 = 0.1188$	$R_1 = 0.0282$, $wR_2 = 0.0675$
Flack			−0.008(10)	

[a] $R_1 = \Sigma||F_o| - |F_c||/\Sigma|F_o|$; $wR_2 = [\Sigma w(F_o^2 - F_c^2)_2/\Sigma w(F_o^2)^2]^{1/2}$.

Table 3. Hydrogen bonds for **1**, **2**, and **4**.

D–H···A	*d*(D–H)	*d*(H···A)	*d*(D···A)	∠DHA	Symmetry code
1					
O2w–H3w···O1	0.820	1.990	2.796	167.32	$[x, -y+1, z+1/2]$
O1w–H2w···O3	0.820	1.958	2.750	162.11	$[-x+1, -y-1, -z+1]$
O1w–H1w···O4	0.839	1.910	2.747	176.28	$[-x+1, y, -z+3/2]$
O2w–H4w···O2	0.868	2.029	2.877	165.40	$[x+1, -y+1, -z+1]$
2					
O1w–H1w···O1	0.798	1.916	2.704	169.06	$[-x+1/2, y-1/2, z]$
4					
O1w–H2wb···O2	0.849	1.794	2.643	179.36	$[-x+1/2, -y+3/2, -z+1]$
O1w–H1wa···N1	0.836	2.059	2.887	171.13	$[-x+1/2, y-1/2, -z+1/2]$
O2w–H2wa···O1	0.807	1.880	2.685	174.43	$[-x+1/2, -y+3/2, -z+1]$
O2w–H2wb···O1	0.743	2.035	2.763	166.57	$[x+1/2, y-1/2, z]$

Downloaded by [Renmin University of China] at 10:42 13 October 2013

3. Results and discussion

3.1. *Crystal structures*

3.1.1. Crystal structure of 1. X-ray crystallography reveals that the asymmetric unit of **1** is composed of one Co^{II}, two fpa^-, and two water molecules (figure 1), with Co^{II} in a disordered octahedral coordination geometry where the basal plane is occupied by three oxygen atoms (O1w, O2, and O3) and N2 from one fpa^- molecule; the axial positions are occupied by one water molecule (O2w) and N1 of fpa^-. Bond angles around Co^{II} range from 82.68(6)° to 171.97(5)°. The Co–O (ranging from 2.0262(14) to 2.1433(14) Å) and Co–N (2.1466(17) and 2.1745(16) Å) bond lengths in **1** are in the expected range for such complexes (table 2). In **1**, each fpa^- coordinates with Co^{II} in μ-(κ^2 *N*, *O*) chelating mode to form a six-membered ring adopting a boatlike, folded conformation. The six-membered ring with largest deviation (0.5830 Å) results in instability due to larger ring strain, so chelation of fpa^- is less stable than the five-membered ring of 2-pyridinecarboxylic acid [23].

$[Co(fpa)_2(H_2O)_2]$ is connected into a 1-D supramolecular single chain by O–H···O hydrogen bonds (O2w–H3w···O1 = 2.796 Å) along the crystallographic *c*-axis (figure 2a). The 1-D supramolecular single chains are joined into a 1-D supramolecular double chain through O–H···O hydrogen bonding (O1w–H1w···O1 = 2.750 Å, O1w–H1w···O4 = 2.747 Å, and O2w–H4w···O2 = 2.877 Å) (figure 2b). Adjacent double chains are further aggregated into a 3-D supramolecular network through π–π interactions between pyridine rings of fpa^- (the closest centroid separation is 3.9587(8) Å with an offset angle of 20.01°) (figure 3).

3.1.2. Crystal structure of 2. The asymmetric unit of **2** contains half a Cu^{II}, one fpa^-, and half a coordinated water molecule (figure 4). Cu and O1w are located in the symmetry plane. Each Cu is distorted square pyramidal, coordinated with two oxygen atoms (O2 and O2a) and two nitrogen atoms (N1 and N1a) from two different fpa^- anions in the equatorial plane; the axial position is occupied by one water molecule (O1w). Due to Jahn–Teller effect of d^9 configuration, the Cu–O1w distance

Table 2. Bond lengths (Å) and angles (°) for **1**–**4**.

1			
Co(1)–O(3)	2.0262(14)	O(1W)–Co(1)–O(2W)	87.64(6)
Co(1)–O(2)	2.0882(14)	O(3)–Co(1)–N(1)	90.11(6)
Co(1)–O(1W)	2.0896(14)	O(2)–Co(1)–N(1)	97.49(6)
Co(1)–O(2W)	2.1433(14)	O(1W)–Co(1)–N(1)	82.68(6)
Co(1)–N(1)	2.1466(17)	O(2W)–Co(1)–N(1)	170.08(6)
Co(1)–N(2)	2.1745(16)	O(3)–Co(1)–N(2)	93.42(6)
O(3)–Co(1)–O(2)	171.97(5)	O(2)–Co(1)–N(2)	87.32(6)
O(3)–Co(1)–O(1W)	90.73(6)	O(1W)–Co(1)–N(2)	172.24(6)
O(2)–Co(1)–O(1W)	87.66(6)	O(2W)–Co(1)–N(2)	85.97(6)
O(3)–Co(1)–O(2W)	87.85(6)	N(1)–Co(1)–N(2)	103.84(6)
O(2)–Co(1)–O(2W)	84.22(6)		
2			
Cu–O(2)	1.9517(14)	O(2)–Cu–N(1)	90.23(7)
Cu–N(1)	2.0218(17)	N(1)#1–Cu–N(1)	175.25(10)
Cu–O(1W)	2.174(2)	O(2)–Cu–O(1W)	94.93(4)
O(2)–Cu–O(2)#1	170.14(9)	N(1)–Cu–O(1W)	92.38(5)
O(2)–Cu–N(1)#1	89.36(7)		
3			
Zn(1)–O(1)	1.949(3)	O(3)–Zn(1)–N(1)	109.55(14)
Zn(1)–O(3)	1.957(3)	O(1)–Zn(1)–N(2)	107.33(14)
Zn(1)–N(1)	2.012(3)	O(3)–Zn(1)–N(2)	114.84(15)
Zn(1)–N(2)	2.022(3)	N(1)–Zn(1)–N(2)	111.18(11)
Zn(2)–O(7)	1.958(3)	O(7)–Zn(2)–O(6)	98.51(13)
Zn(2)–O(6)	1.962(3)	O(7)–Zn(2)–N(5)#2	116.76(14)
Zn(2)–N(5)#2	2.028(3)	O(6)–Zn(2)–N(5)#2	97.96(13)
Zn(2)–N(6)	2.030(3)	O(7)–Zn(2)–N(6)	106.32(15)
O(1)–Zn(1)–O(3)	94.97(11)	O(6)–Zn(2)–N(6)	125.13(16)
O(1)–Zn(1)–N(1)	118.25(15)	N(5)#2–Zn(2)–N(6)	112.18(12)
4			
Zn(1)–O(2W)	2.0850(11)	O(1W)#3–Zn(1)–O(1W)	178.63(6)
Zn(1)–O(1W)	2.0879(10)	O(2W)–Zn(1)–N(2)	91.80(3)
Zn(1)–N(2)	2.1750(15)	O(1W)–Zn(1)–N(2)	89.31(3)
Zn(1)–N(3)	2.2208(15)	O(2W)–Zn(1)–N(3)	88.20(3)
O(2W)#3–Zn(1)–O(2W)	176.39(6)	O(1W)–Zn(1)–N(3)	90.69(3)
O(2W)–Zn(1)–O(1W)#3	87.96(5)	N(2)–Zn(1)–N(3)	180.0
O(2W)–Zn(1)–O(1W)	92.08(5)		

Symmetry transformations used to generate equivalent atoms: #1: $-x+1$ y, $-z+1/2$; #2: $x-2$, y, $z-1$; #3: $-x+1$, y, $-z+1/2$.

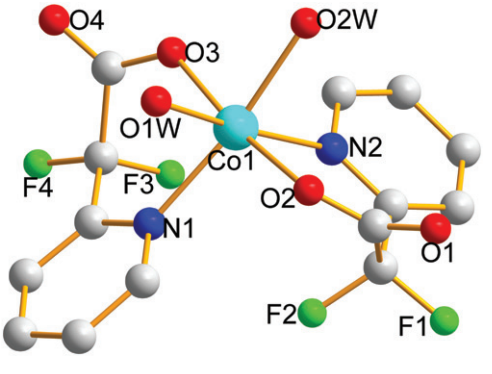

Figure 1. Coordination environment of Co^{II} in **1**.

Downloaded by [Renmin University of China] at 10:42 13 October 2013

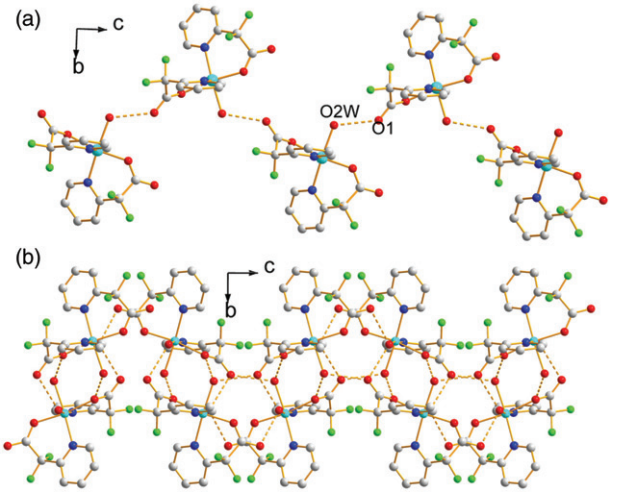

Figure 2. (a) The 1-D supramolecular single chain and (b) 1-D supramolecular double chain along the *c*-axis through hydrogen bonds in **1**. Hydrogen atoms are omitted for clarity.

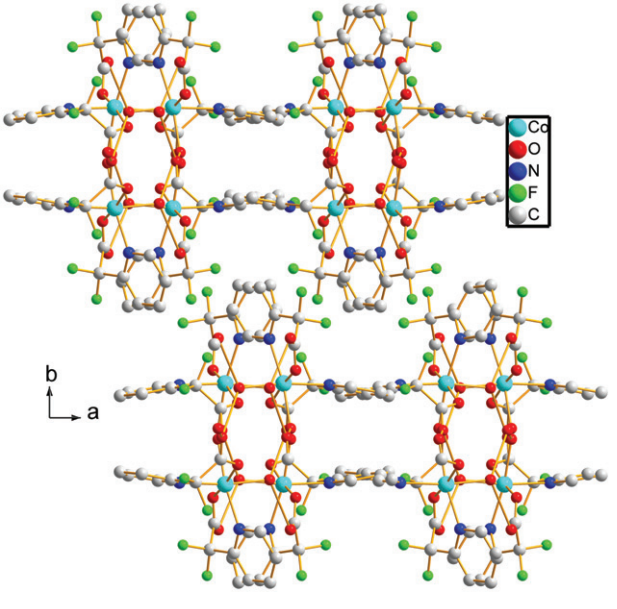

Figure 3. The 3-D supramolecular network *via* $\pi\cdots\pi$ interactions in **1**.

(Cu–O1w = 2.172 Å) is longer than the other Cu–O distances (Cu–O2 = 1.9517(14) Å); the corresponding bond lengths and angles around Cu are listed in table 2, confirming distorted square pyramidal Cu^{II} in **2**. Similar to **1**, fpa^- coordinates with Cu^{II} in μ-(κ^2 *N*, *O*) chelating mode to form a six-membered chelate ring adopting a boatlike, folded conformation with largest deviation of 0.7279 Å.

Downloaded by [Renmin University of China] at 10:42 13 October 2013

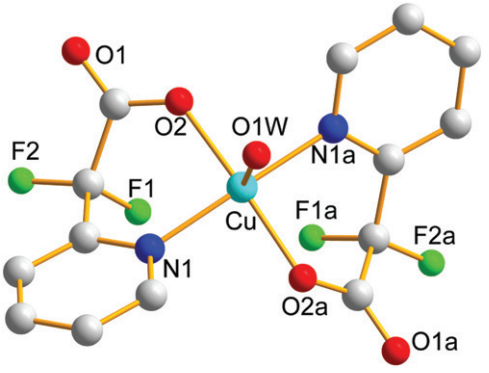

Figure 4. Coordination environment of Cu^{II} in **2**.

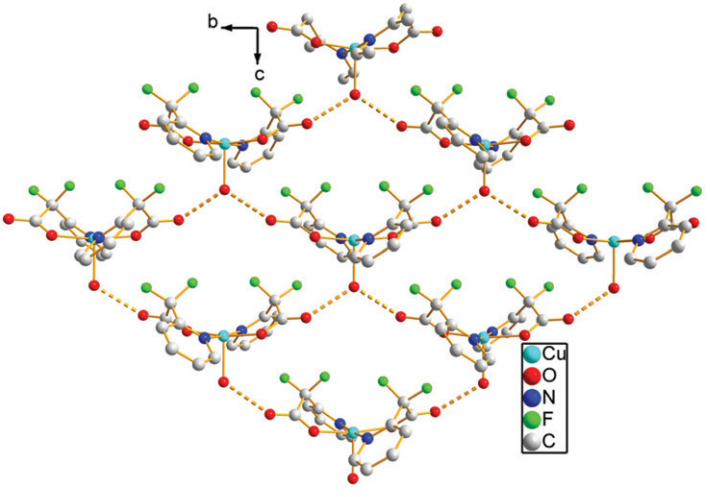

Figure 5. The 2-D supramolecular layer along the *bc*-plane through hydrogen bonds in **2**. Hydrogen atoms are omitted for clarity.

The coordination water is involved in two intermolecular O–H···O hydrogen bonds with uncoordinated carboxyl O1 and O1a from two neighboring molecules to generate a 2-D supramolecular layer with square-grid framework (figure 5), in which four $[Cu(fpa)_2(H_2O)]$ units form eighteen-membered rings. The 2-D layers are packed into a supramolecular network through π–π (the closest centroid separation is 3.9172(7) Å with an offset angle of 17.08°) and F···π interactions (the distance of *F* and aromatic ring of fpa^- is 3.0314 Å) (Supplementary material).

3.1.3. Crystal structure of 3. The asymmetric unit of **3** contains two independent Zn^{II} ions, four fpa^-, and two bpp molecules, in a disordered tetrahedral geometry from two oxygen atoms from two different fpa^- molecules and two nitrogen atoms of two distinct bpp molecules. Bond angles around Zn^{II} range from 94.97(11)° to 125.13(16)°.

Downloaded by [Renmin University of China] at 10:42 13 October 2013

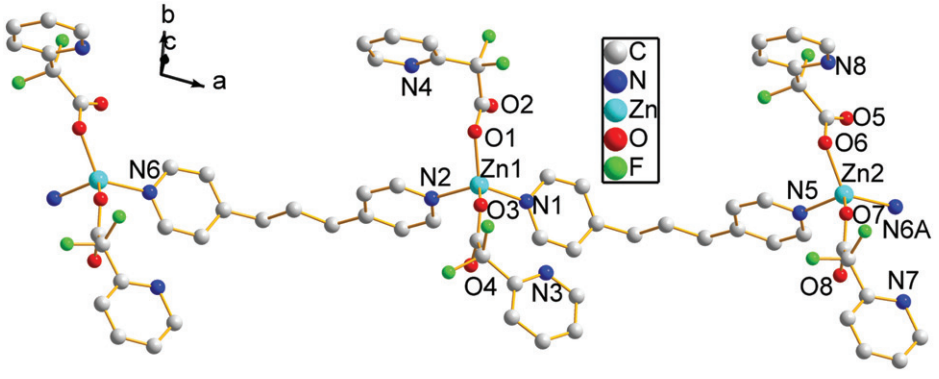

Figure 6. Coordination environment of Zn^{II} in **3**.

The Zn–N (from 2.012(3) to 2.030(3) Å) and Zn–O (from 1.949(3) to 1.962(3) Å) bond lengths in **3** are in expected ranges for Zn^{II} complexes; the bond distances for Zn–N and Zn–O and angle for N/O–Zn–N/O are given in table 2. Complex **2** crystallizes in the chiral space group $P2_1$. Each Zn coordinates with four different ligands (two different bbp molecules in which pyridine rings were perpendicular to one another and two different fpa^- molecules). Because the symmetry of ligands and different conformation are changed by coordination, the chiral space group arises.

In **3**, each bpp links two Zn^{II} centers (Zn1 and Zn2) into a 1-D polymeric chain and fpa^- act as capping ligands in μ-(κ *O*) coordination on two sides of the 1-D chain in an anti-parallel fashion (figure 6). There are four kinds of fpa^- anions (abbreviated to fpa(I), fpa(II), fpa(III), and fpa(IV)) displaying different conformations in **3**. Pyridine rings of fpa(I) containing N11 are parallel with the 1-D chain, fpa(II) containing N10 atom is perpendicular to the 1-D chain, and there is an acute angle between fpa(III) or fpa(IV) and the 1-D chain. The 1-D chains pack into a 3-D supramolecular network through π–π interactions between bpp and fpa (Supplementary material). Only fpa(III) and fpa(IV) are involved in π–π interactions and their closest centroid separations are 3.9436(7) and 4.1834 Å, respectively, with corresponding offset angles of 20.26° and 22.98°.

3.1.4. Crystal structure of 4. X-ray crystallography reveals that the asymmetric unit of **4** is composed of half a Zn^{II}, one uncoordinated fpa^- molecule, 0.5 bpy molecule, and two water molecules, in which Zn^{II} is located in a center of symmetry. Each Zn^{II} shows a slightly distorted octahedral coordination geometry where the basal plane is occupied by four symmetry-related water molecules (O1w and O2w) and the axis is occupied by two nitrogen atoms of two different bpy molecules. The bond lengths of Zn–O/N lie in the range 2.0850(11)–2.2208(15) Å and the corresponding O/N–Zn–O/N bond angles range from 87.96(5)° to 178.63(6)°, indicating distortion of the Zn octahedral geometry. In **4**, each bpy links two $[Zn(H_2O)_4]^{2+}$ units into a 1-D polymeric cationic chain and uncoordinated fpa^- compensate the framework charge (figure 7).

Each O1w is involved in two intermolecular hydrogen bonds (O1w–H1wa···N1 and O1w–H1wb···O2) with two uncoordinated fpa^- molecules which lie on two sides of the

Downloaded by [Renmin University of China] at 10:42 13 October 2013

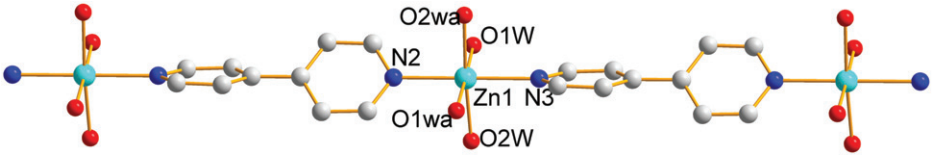

Figure 7. The 1-D cationic polymer chain in **4**.

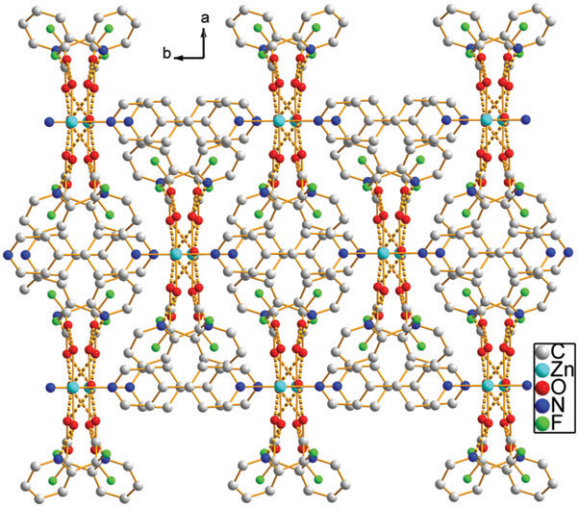

Figure 8. The 3-D packing network of **4** *via* $\pi\cdots\pi$ interactions.

Downloaded by [Renmin University of China] at 10:42 13 October 2013

1-D chain in an anti-parallel fashion to generate a 2-D supramolecular layer with square-grid framework in the *bc*-plane (Supplementary material). Four O1w, two Zn^{II}, and two fpa^- molecules assemble into a puckered 16-membered supramolecular ring *via* hydrogen bonds in the *ac*-plane, in which two O2w molecules and two carboxylate oxygen atoms (O1) protrude. Hydrogen bonds between O2w and O1 stabilize the supramolecular ring; parameters of hydrogen bonds are given in table 3. The 2-D layers were packed into a 3-D supramolecular network through π–π and F$\cdots\pi$ interactions (figure 8).

3.2. *IR spectra of 1–4*

IR spectra of four complexes, shown in Supplementary material, have peaks at 3386 and 2931–2844 cm^{-1} for O–H and C–H stretch of organic linkers. Bands at 1646–1685 cm^{-1} were assigned as asymmetric stretches of carboxylates of fpa^- and 1380–1413 cm^{-1} correspond with symmetric carboxylate stretches. The Deacon–Philips rule is helpful to determine the coordination mode between carboxylates and metal ions by calculating the frequency separation ($\Delta\nu$) between the asymmetric (ν_{as}) and symmetric stretches (ν_s) of the carboxylate [34]. The $\Delta\nu$ for **1**–**4** indicates monodentate

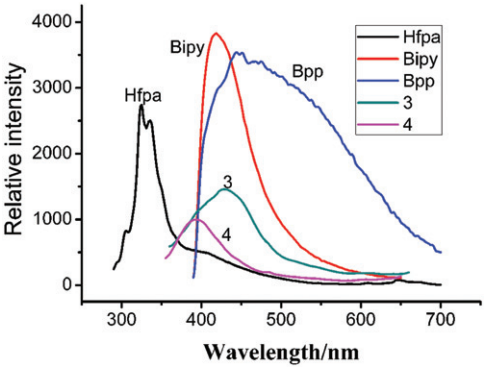

Figure 9. Solid-state emission spectra for Hfpa, bipy, bpp, **3**, and **4** at room temperature.

Downloaded by [Renmin University of China] at 10:42 13 October 2013

or uncoordinated carboxylate for **1**–**4** ($\Delta\nu = 245\,cm^{-1} > 200\,cm^{-1}$, $\nu_{as}(COO^-) = 1655\,cm^{-1}$, $\nu_s(COO^-) = 1410\,cm^{-1}$ for **1**; $\Delta\nu = 306\,cm^{-1} > 200\,cm^{-1}$, $\nu_{as}(COO^-) = 1687\,cm^{-1}$, $\nu_s(COO^-) = 1381\,cm^{-1}$ for **2**; $\Delta\nu = 247\,cm^{-1} > 200\,cm^{-1}$, $\nu_{as}(COO^-) = 1655\,cm^{-1}$, $\nu_s(COO^-) = 1398\,cm^{-1}$ for **3**; $\Delta\nu = 246\,cm^{-1} > 200\,cm^{-1}$, $\nu_{as}(COO^-) = 1646\,cm^{-1}$, $\nu_s(COO^-) = 1400\,cm^{-1}$ for **4**).

3.3. *TG curves of 1–4*

The thermal behaviors of **1**–**4** were studied from 18°C to 700°C under air. The TGAs (Supplementary material) revealed that **1**, **2**, and **4** decomposed through three major processes and **3** decomposed in two major steps. The first loss of **1**, **2**, and **4** corresponded to loss of coordinated water at 70–170°C (7.08% for **1**, 4.62% for **2**, and 11.26% for **4**; the corresponding Calcd 8.20% for **1**, 4.23% for **2**, and 11.29% for **4**). The second weight loss of **1**, **2**, and **4** were characteristic of combustion of parts of fpa^- molecules and the third weight loss corresponded to the residue of fpa and the other ligands. The total weight loss of **1**, **2**, and **4** amounted to 82.13%, 79.88%, and 85.43%, respectively (Calcd. 83.15% for **1**, 81.21% for **2**, and 87.30% for **4**). Similar to **1**, **2**, and **4**, the first weight loss of **3** corresponded to combustion of parts of fpa^- and the second weight loss was characteristic of the combustion of the residue of fpa and bpp. The total weight loss of **3** amounted to 89.94% (Calcd 89.31%). The remaining weights for **1**–**4** correspond to the formation of CoO, CuO, ZnO, and ZnO, respectively (Obsd 17.87% for **1**, 20.12% for **2**, 10.06% for **3**, and 14.57% for **4**, Calcd 16.85% for **1**, 18.79% for **2**, 10.69% for **3**, and 12.70% for **4**).

3.4. *Fluorescence curves of 3 and 4*

The photoluminescence spectra of **3** and **4** as well as Hfpa, bipy, and bpp in the solid state at room temperature are shown in figure 9. Complexes **1** and **2** show very weak luminescence that cannot be detected in the solid state at ambient temperature; both **3** and **4** exhibit blue photoluminescence with emission maxima at 425 and 397 nm upon excitation at 335 and 320 nm, respectively. The photoluminescence spectra of Hfpa, bipy, and bpp revealed intense fluorescent emissions at 330 ($\lambda_{ex} = 280$ nm) for Hfpa,

419 nm for bipy ($\lambda_{ex} = 340$ nm), and 445 nm for bpp ($\lambda_{ex} = 340$ nm). Comparing photoluminescence spectra of ligands and **3**, although the maximum emission wavelength of **3** undergoes a slight blueshift, the emission bands for **3** are very similar to those of free bpp in position and band shape. Therefore, the emissions of **3** may be assigned to $\pi^* \rightarrow \pi$ or $\pi^* \rightarrow n$ transition of bpp ligands [35]. Similarly, emissions of **4** may be due to $\pi^* \rightarrow \pi$ or $\pi^* \rightarrow n$ transition of bipy [36].

3.5. *Discussion*

Although the design and synthesis of target complexes is still a challenge, exploiting a simple system that allows modeling and study of phenomena, which are superimposed upon a more complicated, multi-component system, is helpful to establish general principles. Selection of Efpa as Hfpa source was based on the following consideration: (1) Efpa was easily dissolved in organic solvents such as ethanol, and methanol, providing facility for solvo-thermal reactions; (2) coordination complexes with intriguing structures and wide applications have been successfully obtained *via in situ* hydrolysis of an ester; (3) slow *in situ* formation of Hfpa will ensure growth of single crystals sufficiently large to allow a single-crystal X-ray structure determination; and (4) *in situ* hydrolysis of an ester helps to understand and direct synthesis of target complexes. When Efpa was reacted only with metal salts such as $CuSO_4 \cdot 5H_2O$, $Zn(NO_3) \cdot 4H_2O$, $CoCl_2 \cdot 6H_2O$, $CdCl_2$, or $NiCl_2 \cdot 6H_2O$ under mixed CH_3CH_2OH/H_2O at 85°C, **1** and **2** were easily obtained. Under the help of the second organic linkers such as bpp and bpy, **3** and **4** were obtained; however, only the second linkers (bimb and phen) were involved in coordination with metal ions in **5** and **6**. In **1** and **2**, fpa^- coordinated with metal by a μ-(κ^2 *N*, *O*). However, fewer coordination sites or uncoordinated fpa^- were found in **3** and **4**, respectively. These results revealed the second neutral organic linkers coordinate more readily with metal ions than fpa^- when they are competing. The reasons for formation of fewer coordination sites and uncoordinated fpa^- are: (1) compared with the second organic linker, *in situ* hydrolysis of an ester, which takes some time, results in reduced coordination with metal ions; (2) larger steric hindrance of the second linkers prevents further coordination of fpa^-; and (3) the larger ring strain results in instability of the six-membered ring constructed by chelating fpa^-.

4. Conclusion

By selecting a flexible ligand (Hfpa), four new metal complexes have been isolated and characterized by elemental analyses, IR spectroscopy, single-crystal X-ray diffraction, and TGA. Both **1** and **2** are extended into 3-D supramolecular networks through hydrogen bonds and $\pi \cdots \pi$ interactions. In **3**, bpp molecules link Zn ions into a chain, in which unidentate fpa^- molecules are capping ligands. In **4**, $[Zn(H_2O)_4]^{2+}$ and bpy joined in a 1-D polymeric cationic chain with uncoordinated fpa^- compensating the framework charge. Analyses of syntheses, crystal structures, and coordination modes of fpa^- reveal that neutral linkers are easier to coordinate with metal than fpa^-. TGAs reveal that fpa^- decomposed through two processes.

Downloaded by [Renmin University of China] at 10:42 13 October 2013

Supplementary material

CCDC 860594–860597 for **1**–**4** contain the supplementary crystallographic data. These data can be obtained free of charge from The Cambridge Crystallographic Data Centre *via* http://www.ccdc.cam.ac.uk/data_request/cif

Acknowledgments

This work was supported by the National Natural Science Foundation of China (No.: 21201155), the Natural Science Young Scholars Foundation of Shanxi Province (No.: 2012021007-5), the International Scientific and Technological Cooperation Projects of Shanxi Province (No.: 2011081022), the Natural Science Young Scholars Foundation of North University of China and the Scientific Research Start-up Foundation of North University of China.

Downloaded by [Renmin University of China] at 10:42 13 October 2013

References

[1] M. Eddaoudi, D.B. Moler, H.L. Li, B.L. Chen, T.M. Reineke, M. O'Keeffe, O.M. Yaghi. *Acc. Chem. Res.*, **34**, 319 (2001).
[2] B.J. Holliday, C.A. Mirkin. *Angew. Chem., Int. Ed.*, **40**, 2022 (2001).
[3] B. Moulton, M.J. Zaworotko. *Chem. Rev.*, **101**, 1629 (2001).
[4] O.M. Yaghi, M. O'Keeffe, N.W. Ockwig, H.K. Chae, M. Eddaoudi, J. Kim. *Nature*, **423**, 705 (2003).
[5] S. Kitagawa, R. Kitaura, S. Noro. *Angew. Chem., Int. Ed.*, **43**, 2334 (2004).
[6] G. Ferey. *Chem. Soc. Rev.*, **37**, 191 (2008).
[7] J.R. Li, R.J. Kuppler, H.C. Zhou. *Chem. Soc. Rev.*, **38**, 1477 (2009).
[8] L.Q. Ma, C. Abney, W.B. Lin. *Chem. Soc. Rev.*, **38**, 1248 (2009).
[9] D.J. Tranchemontagne, J.L. Mendoza-Cortes, M. O'Keeffe, O.M. Yaghi. *Chem. Soc. Rev.*, **38**, 1257 (2009).
[10] R. Chakrabarty, P.S. Mukherjee, P.J. Stang. *Chem. Rev.*, **111**, 6810 (2011).
[11] A. Corma, H. García, F.X. Llabrès i Xamena. *Chem. Rev.*, **111**, 4607 (2011).
[12] J.P. Zhang, Y.B. Zhang, J.B. Lin, X.M. Chen. *Chem. Rev.*, **112**, 1001 (2012).
[13] J.R. Li, J.L. Sculley, H.C. Zhou. *Chem. Rev.*, **112**, 869 (2012).
[14] T.L. Hennigar, D.C. MacQuarrie, P. Losier, R.D. Rogers, M.J. Zaworotko. *Angew. Chem., Int. Ed.*, **36**, 972 (1997).
[15] A.J. Blake, N.R. Brooks, N.R. Champness, P.A. Cooke, A.M. Deveson, D. Fenske, P. Hubberstey, W.S. Li, M. Schroder. *J. Chem. Soc., Dalton Trans.*, 2103 (1999).
[16] C.Y. Su, Y.P. Cai, C.L. Chen, M.D. Smith, W. Kaim, H.C. zur Loye. *J. Am. Chem. Soc.*, **125**, 8595 (2003).
[17] S.C. Chen, Z.H. Zhang, K.L. Huang, Q. Chen, M.Y. He, A.J. Cui, C. Li, Q. Liu, M. Du. *Cryst. Growth Des.*, **8**, 3437 (2008).
[18] B.R. Manzano, F.A. Jalon, M.L. Soriano, M.C. Carrion, M.P. Carranza, K. Mereiter, A.M. Rodriguez, A. de la Hoz, A. Sanchez-Migallon. *Inorg. Chem.*, **47**, 8957 (2008).
[19] T.K. Prasad, M.V. Rajasekharan. *Cryst. Growth Des.*, **8**, 1346 (2008).
[20] G.J.T. Cooper, G.N. Newton, D.L. Long, P. Kogerler, M.H. Rosnes, M. Keller, L. Cronin. *Inorg. Chem.*, **48**, 1097 (2009).
[21] N. Stock, S. Biswas. *Chem. Rev.*, **111**, 933 (2012).
[22] U. Bierbach, M. Sabat, N. Farrell. *Inorg. Chem.*, **39**, 1882 (2000).
[23] S.Y. Desjardins, K.J. Cavell, H. Jin, B.W. Skelton, A.H. White. *J. Organomet Chem.*, **515**, 233 (1996).
[24] X.M. Li, Y.L. Niu, Q.W. Wang, B. Liu, X. Zhao, D. Li. *Chin. J. Struct. Chem.*, **28**, 321 (2009).
[25] M. Tabatabaee, F. Abbasi, B.M. Kukovec, N. Nasirizadeh. *J. Coord. Chem.*, **64**, 1718 (2011).
[26] F.M. Nie, J. Chen, Z. Li, F. Lu. *J. Coord. Chem.*, **63**, 1711 (2010).
[27] J. Li, D. Li, L. Tang, Y. Wu, W. Wang, Y. Wang. *J. Coord. Chem.*, **61**, 2916 (2008).
[28] J.G. Małecki, J. Kusz. *J. Coord. Chem.*, **60**, 2461 (2007).

[29] R. Berger, G. Resnati, P. Metrangolo, E. Weberd, J. Hulliger. *Chem. Soc. Rev.*, **40**, 3496 (2011).
[30] J.Y. Sun, X.D. Tong, H.Z. Xu. *Inorg. Chem. Commun.*, **13**, 645 (2010).
[31] J. Zhang, J.F. Song. *Acta E*, **67**, m1633 (2011).
[32] G.M. Sheldrick. *SHELXS 97, Program for Crystal Structure Refinement*, University of Göttingen, Göttingen (1998).
[33] A.L. Spek. *PLATON, Molecular Geometry Program*, University of Utrecht, The Netherlands (1999).
[34] G.B. Deacon, R. Phillips. *Coord. Chem. Rev.*, **33**, 227 (1980).
[35] Y.Q. Zheng, J. Zhang, J.Y. Liu. *CrystEngComm*, **12**, 2740 (2010).
[36] C.F. Yan, F.L. Jiang, L. Chen, R. Feng, M. Yang, M.C. Hong. *J. Solid State Chem.*, **182**, 3162 (2009).

Downloaded by [Renmin University of China] at 10:42 13 October 2013